

1 **Splenic autonomic denervation increases inflammatory status, but**
2 **does not aggravate atherosclerotic lesion development**

3
4 Sander Kooijman^{1,2*#}, Illiana Meurs^{1,2*}, Lianne van Beek^{2,3}, P. Padmini S.J. Khedoe⁴, Annabel
5 Giezekamp^{1,2}, Karin Pike-Overzet⁵, Cathy Cailotto⁶, Jan van der Vliet⁶, Vanessa van
6 Harmelen^{2,3}, Guy Boeckxstaens⁶, Jimmy F.P. Berbée^{1,2} and Patrick C.N. Rensen^{1,2}

7
8 ¹Department of Medicine, Division of Endocrinology, Leiden University Medical Center, Leiden,
9 the Netherlands, ²Eindhoven Laboratory for Experimental Vascular Medicine, Leiden University
10 Medical Center, Leiden, the Netherlands, ³Department of Human Genetics, Leiden University
11 Medical Center, Leiden, the Netherlands, ⁴Department of Pulmonology, Leiden University
12 Medical Center, Leiden, the Netherlands, ⁵Department of Immunohematology and Blood
13 Transfusion, Leiden University Medical Center, Leiden, the Netherlands, ⁶Department of
14 Gastroenterology & Hepatology, Academic Medical Center Amsterdam, the Netherlands.

15

16 *Both authors contributed equally

17

18 Short title: Splenic denervation, inflammation and atherosclerosis

19

20 #Corresponding author: Sander Kooijman, Department of Endocrinology, post zone C7Q, Leiden
21 University Medical Center, P.O. Box 9600, 2300 RC Leiden, The Netherlands. Phone: +31-71-
22 52-68166. Email: s.kooijman@lumc.nl

23

24 Keywords: Atherosclerosis, inflammation, splenic denervation, transgenic mice

25

26 **Abstract**

27 **Objective:** The brain plays a prominent role in the regulation of inflammation. Immune cells are
28 under control of the so-called cholinergic anti-inflammatory reflex, mainly acting via autonomic
29 innervation of the spleen. Activation of this reflex inhibits the secretion of pro-inflammatory
30 cytokines and may reduce the development of atherosclerosis. Therefore, the aim of this study
31 was to evaluate the effects of selective parasympathetic (Px) and sympathetic (Sx) denervation
32 of the spleen on inflammatory status and atherosclerotic lesion development.

33 **Methods & Results:** Female APOE*3-Leiden.CETP mice, a well-established model for human-
34 like lipid metabolism and atherosclerosis, were fed a cholesterol-containing Western-type diet
35 for 4 weeks after which they were sub-divided into three groups receiving either splenic Px,
36 splenic Sx or sham surgery. The mice were subsequently challenged with the same diet for an
37 additional 15 weeks. Selective Px increased leukocyte counts (i.e. dendritic cells, B cells and T
38 cells) in the spleen and increased gene expression of pro-inflammatory cytokines in the liver and
39 peritoneal leukocytes as compared to Sx and sham surgery. Both Px and Sx increased
40 circulating pro-inflammatory cytokines IL-1 β and IL-6. However, the increased pro-inflammatory
41 status in denervated mice did not affect atherosclerotic lesion size or lesion composition.

42 **Conclusion:** Predominantly selective Px of the spleen enhances the inflammatory status, which
43 however does not aggravate diet-induced atherosclerotic lesion development.

44

45 **New & Noteworthy statement**

46 Splenic immune cells are involved atherosclerosis development and their inflammatory status is
47 controlled by the anti-inflammatory reflex. Here we show that both selective sympathetic and
48 parasympathetic denervation of the spleen results in enhanced pro-inflammatory cytokine
49 production, but does not aggravate atherosclerosis development.

50

51 **Introduction**

52 Atherosclerosis is a chronic inflammatory disease initiated by innate and adaptive immune
53 responses to endogenously modified structures, in particular oxidized lipoproteins, within the
54 arterial wall (8). The autonomic nervous system may enhance innate immune responses by
55 sympathetic activity (reviewed in 12), while it suppresses inflammation via the vagus nerve, a
56 mechanism termed the cholinergic anti-inflammatory pathway (3; 7). In response to circulating
57 pro-inflammatory cytokines afferent vagal nerves are directly activated. Subsequent efferent
58 vagal activity results in the release of acetylcholine which activates the $\alpha 7$ nicotinic acetylcholine
59 receptor ($\alpha 7$ nAChR) on resident tissue macrophages and other immune cells, thereby inhibiting
60 the production and release of pro-inflammatory cytokines (e.g. TNF α , IL-6, IL-1 β) (24). $\alpha 7$ nAChR
61 is integral to the cholinergic anti-inflammatory pathway, as vagus nerve stimulation fails to inhibit
62 TNF α production in pharmacologically $\alpha 7$ nAChR inhibited or $\alpha 7$ nAChR-deficient mice (18; 24).
63 Recently, we demonstrated that hematopoietic $\alpha 7$ nAChR deficiency in dyslipidemic mice
64 enhances systemic inflammation as evidenced by increased leukocytes in the blood, lymph
65 nodes, spleen and peritoneum (all by at least 2-fold) and increased gene expression of TNF α in
66 peritoneal leukocytes and spleen (15).

67 As the spleen contains half of the body's monocyte population, it is not surprising that the
68 cholinergic anti-inflammatory pathway acts mainly via the spleen. Indeed, Huston *et al.* (11)
69 reported that vagus nerve stimulation fails to inhibit TNF α production in splenectomised animals
70 during endotoxemia, indicating an essential role for the spleen in the cholinergic anti-
71 inflammatory pathway. Furthermore, splenectomy reduces the production of antibodies directed
72 against oxidized LDL in apoE-deficient mice and was associated with increased atherosclerotic
73 lesion development (16). Trauma patients who undergo splenic removal are more prone to
74 develop coronary heart disease, in which enhanced atherosclerotic lesion development may be
75 causal (17).

76 Taken together, these findings suggests that autonomic innervation of the spleen and the
77 development of atherosclerosis may be closely interrelated. Therefore, the aim of this study was
78 to determine the effect of selective parasympathetic denervation (Px), as compared to
79 sympathetic denervation (Sx) of the spleen and sham surgery, on systemic inflammation and
80 atherosclerotic lesion development in female APOE*3-Leiden.CETP mice, a well-established
81 mouse model for human-like lipoporotein metabolism.

82

83 **Material and Methods**

84

85 **Animals**

86 APOE*3-Leiden mice were crossbred with mice expressing human cholesteryl ester transfer
87 protein (CETP) under control of its natural flanking regions to generate heterozygous APOE*3-
88 Leiden.CETP mice (25). Mice were housed under standard conditions with a 12:12h light:dark
89 cycle and had free access to food and water. At the age of 10-12 weeks, female APOE*3-
90 Leiden.CETP mice received a Western-type diet (WTD) containing 0.1% cholesterol (w/w), 1%
91 (w/w) corn oil and 15% (w/w) cacao butter (AB diets, Woerden, the Netherlands). After a run-in
92 period of 4 weeks, mice (n=45) were randomized based on plasma lipid levels and body weight
93 into three groups (n=15 each) receiving either splenic parasympathetic denervation (Px), splenic
94 sympathetic denervation (Sx) or sham surgery. A schematic representation of the innervation of
95 the spleen and the sites of denervation can be found in **Fig. 1A**. For all surgeries, mice were
96 anesthetized by an intraperitoneal (i.p.) injection of a mixture of fentanyl/citrate/fluanisone
97 (Hypnorm; Janssen, Beerse, Belgium), midazolam (Dormicum; Roche, Mijdrecht, The
98 Netherlands), and H₂O (1: 1: 2, v/v). All animal experiments had been approved by the
99 Institutional Ethics Committee on Animal Care and Experimentation.

100

101 **Selective parasympathetic denervation of the spleen**

102 Since parasympathetic nerves enter the spleen at both tips, these tips were sequentially
103 exposed during surgery to allow cutting of the nerves. After a midline abdominal incision the
104 spleen was pulled gently towards the site of the incision, and the nerve at the tip of the spleen
105 was cut. The connective tissue between the tip and the first hilus was also removed, as some
106 parasympathetic input reaches the spleen via this connective tissue. Subsequently, the spleen
107 was further pulled towards the midline to reach the lower tip of the spleen. After following back

108 the nerve to the plexus, the connective tissue from this plexus back to the spleen was removed.
109 The wound was closed with novosyn suture (B. Braun Medical, Oss, The Netherlands) (5).

110
111 **Selective sympathetic denervation of the spleen**
112 A midline abdominal incision was performed along the linea alba and the stomach was pushed
113 up and to the right to reveal the blood vessels to and from the spleen. After the arterial branch to
114 the stomach a bifurcation indicates the first branching point of the arterial supply to the spleen.
115 From this bifurcation on the arteries will split many times and end at the hili of the spleen.
116 Sympathetic nerves run along and around these arteries to reach the spleen. The area just
117 before and after the bifurcation was chosen to remove the sympathetic nerves. The wound was
118 closed with novosyn suture (B. Braun Medical, Oss, The Netherlands) (5). Sympathetic
119 denervation was confirmed 15 weeks after surgery by Western blotting for tyrosine hydroxylase
120 (TH; anti-TH antibody; AB-112; Abcam).

121
122 **Gene expression analysis in spleen, liver and peritoneal leukocytes**
123 After surgery, the mice were fed the WTD for another 15 weeks. Subsequently, mice were
124 sacrificed and organs were collected and peritoneal leukocytes isolated by lavage of the
125 peritoneum with ice-cold PBS. Total RNA from spleen, liver and peritoneal leukocytes was
126 isolated using the Nucleospin RNA II kit (Macherey-Nagel, Düren, Germany) according to
127 manufacturer's instructions. One microgram of total RNA was converted to cDNA with iScript
128 cDNA Synthesis kit (Biorad) and purified with Nucleospin Extract II kit (Macherey-Nagel). Real-
129 time polymerase chain reaction (RT-PCR) was conducted on the IQ5 PCR machine (Biorad)
130 using the Sensimix SYBR Green RT-PCR mix (Quantace, London, UK). mRNA levels were
131 normalized to mRNA levels of $\beta 2$ microglobulin, cyclophilin, and acidic ribosomal
132 phosphoprotein P0 (36B4).

133

134 **Flow cytometry analysis**

135 From five randomly selected animals per group, peripheral blood and spleens were processed
136 for flow cytometry. Thereto, single cell suspensions were obtained by mashing the cells trough a
137 70 µm cell strainer (Falcon, The Netherlands). Subsequently, cells were counted and 2×10^6 cells
138 were stained with appropriate antibodies (**Table 1**) to determine immune cell subsets: Live
139 immune cells were selected from the forward and sideward scatter, and populations of B cells
140 (CD19+), dendritic cells (CD11c+CD14-), T cells (CD3+), neutrophils (CD11b+Ly6G^{high}) , and
141 macrophages (CD14+CD11b+) were identified. Specific T cell subsets were determined within
142 the CD3+ fraction as T helper cells (CD4+), cytotoxic T cells (CD8+), activated T cells (CD25+),
143 naïve T cells (CD62L+). Data were acquired on a FACSAria or a FACSCanto II (BD
144 Biosciences). Analyses were performed using FlowJo software (Treestar, Ashland, OR, USA).
145 Gating strategy is shown in **Fig. 1B**.

146

147 **Serum measurements**

148 Serum was isolated and stored frozen at -80°C until further analyses. The cytokines TNF α , IL-1 β
149 and IL-6 were determined using V-PLEX Proinflammatory Panel1 (mouse) Kit (Meso Scale
150 Discovery, Rockville, ML, USA) according to the manufacturer's instructions. In 50x diluted
151 serum samples, E-selectin concentrations were measured according to the manufacturer's
152 instructions (DY575, R&D systems, Minneapolis, MN, USA).

153

154 **Plasma lipid and lipoprotein analyses**

155 Blood was collected after a 4-h fast into EDTA-containing cups by tail bleeding, and plasma was
156 isolated by centrifugation and stored frozen at -80°C until further analyses. The concentrations
157 of total cholesterol (TC) and triglycerides (TG) in plasma were determined using commercially
158 available enzymatic colorimetric kits according to the manufacturer's protocols (236691 and
159 1488872; Roche Molecular Biochemicals, Indianapolis, IN, USA). The concentrations of

160 phospholipids (PL) in plasma were determined using a commercially available enzymatic
161 colorimetric kit (3009; Instruchemie, Delfzijl, The Netherlands). The distribution of lipids over the
162 different lipoproteins in plasma was determined after fractionation of pooled plasma (14-15 mice
163 per pool) by FPLC using a Superose 6 HR 10/30 column (Äkta System; Amersham Pharmacia
164 Biotech, Piscataway, NJ).

165

166 **Atherosclerosis quantification**

167 From all mice, hearts were isolated and fixed in phosphate-buffered 4% formaldehyde,
168 dehydrated and embedded in paraffin. Cross-sections (5 μm) were made throughout the aortic
169 root area and stained with hematoxylin-phloxine-saffron for histological analysis. Lesions were
170 categorized for severity according to the guidelines of the American Heart Association adapted
171 for mice (27). Various types of lesions were discerned: no lesions, mild lesions (types 1-3) and
172 severe lesions (types 4-5). Immunohistochemistry for determination of lesion composition was
173 performed as described previously (10). Rat anti-mouse antibody MAC3 (1:1000; BD
174 Pharmingen, Breda, The Netherlands) was used to quantify macrophage area. Monoclonal
175 mouse antibody M0851 (1:800; Dako, Heverlee, the Netherlands) against smooth muscle cell
176 (SMC) α -actin was used to quantify SMC area. Sirius Red was used to quantify collagen area.
177 Lesion area was quantified in the aortic root starting from the appearance of open aortic valve
178 leaflets in four subsequent sections with 50 μm intervals. In ImageJ the lesions were delineated
179 to determine mean lesion area (in μm^2) and a color threshold was set to determine the area
180 percentage of MAC3, SMC or collagen staining in a consistent manner across the different
181 slides.

182

183 **Statistical analysis**

184 Data are presented as means \pm SEM unless indicated otherwise. To compare differences
185 among groups one-way ANOVA with Turkey's post-test was performed using GraphPad Prism

186 version 4.00 for Windows (GraphPad Software, San Diego, CA, USA, www.graphpad.com).

187 Differences at a P-value <0.05 were considered statistically significant.

188

189 **Results**

190 Female APOE*3-Leiden.CETP mice were fed a WTD during 4 weeks, and were randomized into
191 three groups receiving either parasympathetic denervation (Px) of the spleen, sympathetic
192 denervation (Sx) of the spleen (**Fig. 1A**), or sham surgery. After surgery, the mice received WTD
193 feeding for 15 additional weeks to induce atherosclerotic lesion development. To confirm that Sx
194 was successful and that sympathetic nerves did not regenerate, tyrosine hydroxylase (TH)
195 content of the spleen was determined (**Fig. 1C**), showing the absence of TH still 15 weeks after
196 Sx. Upon sacrifice of the mice, the tips of the spleen were gently exposed to confirm that the
197 re-innervation of the parasympathetic nerves was not the case.

198

199 **Splenic parasympathetic denervation increases immune cell count in spleen**

200 The spleen plays an important role in the immune system and, therefore, contains a wide range
201 of immune cell types, including monocytes, macrophages, dendritic cells, neutrophils, T cells
202 and B cells. To define the effect of the selective denervations on immune cell composition, flow
203 cytometry analyses were performed. Total splenic immune cell count was increased (+49%,
204 $p < 0.01$) in Px mice ($200 \pm 10 \times 10^6$ cells) compared to sham operated mice ($134 \pm 10 \times 10^6$ cells),
205 while Sx denervation did not affect immune cell count ($156 \pm 25 \times 10^6$ cells) (**Fig. 2A**). In a fraction
206 of immune cells (i.e. 2.0×10^6 cells), percentages of each cell type were analyzed using flow
207 cytometry and multiplied with total immune cell counts (see Fig. 1B for the gating strategy). This
208 revealed an increase in the number of various immune cell subtypes, including B cells (98 ± 7
209 $\times 10^6$ cells vs. $61 \pm 5 \times 10^6$ cells, $p < 0.01$) (**Fig. 2B**), T cells ($63 \pm 4 \times 10^6$ cells vs. $41 \pm 4 \times 10^6$ cells,
210 $p < 0.01$) (**Fig. 2C**) and dendritic cells (DCs; $10 \pm 1 \times 10^6$ cells vs. $7 \pm 1 \times 10^6$ cells, $p < 0.05$) (**Fig. 2D**).
211 Neutrophils (**Fig. 2E**) and monocytes/macrophages (**Fig. 2F**) only showed a non-significant
212 increase upon Px.

213 As T cells are probably involved in the propagation of nerve signals towards monocytes
214 and macrophages (19), the phenotype of the T cells (i.e naivity or activation status of the T
215 helper or cytotoxic T cells) was further studied. In accordance to the general increase in various
216 immune cells, Px increased both T-helper (T_H ; +60%, $p<0.01$) (**Fig. 2G**) and cytotoxic T cells
217 (T_{cyt} ; +49%, $p<0.01$) (**Fig. 2H**). Further subdivision revealed that Px increased naïve (**Fig. 2I**) as
218 well as activated (**Fig. 2J**) T_H cells, and increased naïve T_{cyt} cells (**Fig. 2K**) without increasing
219 activated T_{cyt} cells (**Fig. 2L**). Thus, splenic Px resulted in an overall increase in immune cells in
220 the spleen, while Sx did not affect immune cell count compared to sham surgery, indicating the
221 importance of the parasympathetic nerve in regulation of the immune system.

222

223 **Splenic autonomic denervation increases expression of inflammatory cytokines**

224 During the course of the experiment, body weight gain was slightly lower in both Px and Sx
225 mice. At the end of the experiment, body weight of sham operated mice was 31.6 ± 1.1 g,
226 compared to 27.3 ± 1.1 g ($p<0.05$) and 27.4 ± 1.2 g ($p<0.05$) for Px and Sx mice, respectively
227 (**Fig. 3A**). Splenic weight tended to be increased in Px (**Fig. 3B**) and was different when
228 expressed as percentage of the body weight for Px (0.52 ± 0.02 %; $p<0.001$) and Sx (0.47 ± 0.02
229 %; $p<0.05$) compared to sham (0.41 ± 0.01 %) (**Fig. 3C**). Gene expression analyses revealed
230 that Px only caused a trend towards an increase of the inflammatory cytokines IL-1 β and IL-6
231 within the spleen (**Fig. 3D**). Further analysis of other organs showed no difference in liver weight
232 when expressed as percentage of the body weight (**Fig. 3E**). Interestingly, Px increased gene
233 expression of IL-6 in the liver (+80%; $p<0.01$) (**Fig. 3F**) and increased gene expression of TNF α ,
234 IL-1 β and IL-6 in isolated peritoneal leukocytes, which reached significance for IL-1 β (3.3-fold;
235 $p<0.05$) (**Fig. 3G**). Next we determined the effect of Px on white blood cell count in peripheral
236 blood and further analysed subsets by flow cytometry. Px tended to increase total immune cell
237 count albeit significance was not reached (+41%; $p=0.18$) (**Fig. 4A**). Subdivision of leukocytes
238 into B cells (**Fig. 4B**), T cells (**Fig. 4C**), dendritic cells (**Fig. 4D**), neutrophils (**Fig. 4E**) or

239 monocytes (**Fig. 4F**) did not reveal differences. However, as the number of immune cells per se
240 does not reflect activity of these cells, we measured serum levels of TNF α (**Fig. 4G**), IL-1 β (**Fig.**
241 **4H**) and IL-6 (**Fig. 4I**) in serum. While TNF α levels remained unaffected, both IL-1 β and IL-6
242 serum concentrations were increased by Px. Interestingly, in contrast to our gene expression in
243 liver, spleen and peritoneal leukocytes, also Sx increased inflammatory status as IL-1 β and IL-6
244 levels compared to sham operated mice.

245

246 **Splenic autonomic denervation does not affect atherosclerotic lesion development**

247 Since inflammation can influence lipid metabolism (22), we next evaluated whether selective
248 splenic denervations had an effect on lipid metabolism. Plasma total cholesterol (TC),
249 phospholipids (PL) and triglycerides (TG) were assessed at 2, 4, 6 and 15 weeks after surgery.
250 No differences in plasma lipid concentrations were found between the Px, Sx and sham
251 operated mice at weeks 2, 4, 6 (not shown) and 15 weeks (**Fig. 4J**). Likewise, the distribution of
252 cholesterol over the various lipoproteins did not differ between Px, Sx or sham control mice (**Fig.**
253 **4K**). Serum E-selectin as marker for vascular inflammation, was increased in Px as well as in Sx
254 compared to sham, suggesting that immune cell infiltration into atherosclerotic lesions might be
255 enhanced by the selective denervations (**Fig 4L**).

256 To study the effect of splenic denervation on atherosclerosis development, mice were
257 sacrificed after 15 weeks after surgery, and atherosclerotic lesion size and lesion severity were
258 determined in the valve area of the aortic root. Both Px and Sx did neither affect atherosclerotic
259 lesion size (**Fig. 5A** and **5B**) nor lesion severity, when classified as mild (type 1-3) and severe
260 (type 4-5) lesions (**Fig. 5C**). However, also no significant differences were observed in lesion
261 composition between Px, Sx and sham operated mice, with respect to the relative area of
262 smooth muscle cells (SMC; α -actin staining; **Fig. 5D**), collagen (Sirius Red staining; **Fig. 5E**) and
263 macrophages (MAC3 staining; **Fig. 5F**).

264

265 **Discussion**

266 In the current study, we tested the hypothesis that the brain plays a prominent role in modulating
267 the activity of immune cells and may therefore affect atherosclerosis development. We
268 determined the effect of selective splenic parasympathetic denervation (Px), sympathetic
269 denervation (Sx) on the inflammatory status and examined the potential consequences for
270 plasma lipids and the development of atherosclerosis in APOE*3-Leiden.CETP mice. We
271 showed that predominantly splenic Px increased the inflammatory state of the body as indicated
272 by increased leukocyte counts within the spleen and increased pro-inflammatory cytokine
273 expression. However, splenic Px as well as Sx did not affect atherosclerotic lesion development.

274 Interestingly, we found increased circulating levels of the pro-inflammatory cytokines IL-
275 1 β and IL-6 upon both Px and Sx. Classically, the parasympathetic and sympathetic nerves
276 system act in opposite direction to facilitate control over physiological responses to maintain
277 homeostasis. However, for the spleen, it has been suggested that both systems in fact act
278 together to restrain inflammation by projection of the vagus nerve also onto the sympathetic
279 splenic nerve (18; 23). Previous studies even suggested absence of direct parasympathetic
280 innervation of the spleen as neither choline acetyltransferase nor vesicular acetylcholine
281 transporter producing nerve endings could be detected within the spleen (2; 18). However the
282 absence of the classical vagus transmitter acetylcholine is not sufficient proof for the absence of
283 direct input from the vagus. In previous studies we identified neuronal connections between the
284 spleen and both the intermedio lateral column of the spinal cord (IML) and the dorsal motor
285 nucleus of the vagus nerve (DMV) by retrograde tracing using pseudorabies virus (PRV) and
286 cholera toxin-b (CTB) (5; 6), suggesting sympathetic as well as parasympathetic neuronal
287 connectivity. Surgical ablation of the nerves along the splenic arteries (similar to Sx) resulted in
288 undetectable retrograde tracer in the IML and absence of TH in the spleen. In contrast, surgical
289 ablation of the nerve branches at the splenic ends (similar to Px) resulted in a loss of

290 detectability of the tracers in the DMV and can therefore most likely be allocated to the
291 parasympathetic nerves system. In addition, Px severely diminished (-70%) LPS-induced
292 antibody production, clearly indicating functional involvement of these nerve branches in the
293 control of the immune response (5). In contrast, Sx did not affect the production of specific
294 antibodies. While absence of sympathetic input 15 weeks after Sx was confirmed by measuring
295 TH content, confirmation of Px was limited to visual inspection due to the lack of specific
296 markers for these neurons. However, consistent with the notion that vagal activation suppresses
297 the immune response (24), we found that Px enhances the number of leukocytes and increases
298 expression of pro-inflammatory cytokines. It may seem contradictory that Px results in
299 diminished LPS-induced antibody production (5), while here we report enhanced inflammatory
300 responses. However, one should consider the dual challenge for the brain during inflammation,
301 namely to contain the inflammation by for example reducing cytokine production, and
302 subsequently to induce memory within the immune system to prevent new infections by inducing
303 antibody production.

304 Despite that Px increased the number of immune cells in the spleen in the current study,
305 no differences in splenic TNF α gene expression or circulating TNF α levels were found. Possibly
306 stronger inflammatory stimuli are required to attenuate TNF α production by spleen macrophages
307 via stimulation of the vagus nerve, as has been shown for LPS-induced endotoxemia (18).
308 Compatible with the notion that TNF α is crucially involved in the pathogenesis and progression
309 of atherosclerosis (4; 14), Px and Sx did not aggravate WTD-induced atherosclerotic lesion
310 development and did not affect lesion composition in APOE*3-Leiden.CETP mice. Similarly, we
311 previously showed that hematopoietic α 7nAChR deficiency in ApoE^{-/-} mice does increase
312 inflammatory status of the body and enhances platelet reactivity, but does not aggravate
313 atherosclerosis as lesion size and plaque composition remained unaffected (15). In contrast,
314 Johansson *et al.* (13) recently reported an increase in atherosclerotic lesion development upon
315 hematopoietic α 7nAChR deficiency in Ldlr^{-/-} mice, indicating that the genetic and environmental

316 context are important to determine the outcome of disrupted anti-inflammatory reflexes. Despite
317 conflicting outcomes, interfering with inflammatory reflexes might be an interesting target in the
318 prevention of atherosclerosis. Several animal studies report beneficial effects of low dose β -
319 blockers on atherogenesis (20; 21), mainly via reducing of inflammatory responses rather than
320 changes in lipid metabolism. Also in humans, the use of metoprolol slows progression of intima-
321 media thickness (9; 26).

322 While the role of the autonomic splenic nerves in human physiology is unclear,
323 splenectomy in trauma patients has been associated with frequency of ischemic coronary
324 diseases, probably explained by increased plasma lipids (17). Rodent studies confirmed the role
325 of the spleen in lipid metabolism as splenectomized rats showed reduced HDL-cholesterol and
326 increased plasma triglycerides. Complete removal of the spleen in ApoE-deficient mice
327 increased plaque development, although the underlying mechanism remained elusive (16). In
328 the current study, no differences in plasma lipids were found upon splenic denervations,
329 suggesting that regulation of lipid metabolism via the spleen is probably not mediated via
330 innervation of the splenic nerves, which may explain why atherosclerosis development was not
331 aggravated in this study. Interestingly, splenectomized trauma patients do display increased
332 infection rates and have increased leukocyte counts (1), corresponding with the data presented
333 in the current study, however the exact contribution of an isolated increased inflammatory status
334 without effects on plasma lipid levels to atherosclerosis development is unclear.

335 In conclusion, selective disruption of mainly the splenic parasympathetic nerve increases
336 splenic immune cell counts and the systemic inflammatory status, but does not contribute to
337 atherosclerotic lesion development.

338

339

340 **Acknowledgements**

341 P.C.N. Rensen is an Established Investigator of the Netherlands Heart Foundation (grant
342 2009T038).

343

344 **References**
345
346 1. Guidelines for the prevention and treatment of infection in patients with an absent or
347 dysfunctional spleen. *BMJ* 312: 430-434, 1996.
348 2. **Berthoud HR and Powley TL**. Interaction between parasympathetic and sympathetic
349 nerves in prevertebral ganglia: morphological evidence for vagal efferent innervation of
350 ganglion cells in the rat. *Microsc Res Tech* 35: 80-86, 1996.
351 3. **Borovikova LV, Ivanova S, Zhang M, Yang H, Botchkina GI, Watkins LR, Wang H,**
352 **Abumrad N, Eaton JW and Tracey KJ**. Vagus nerve stimulation attenuates the systemic
353 inflammatory response to endotoxin. *Nature* 405: 458-462, 2000.
354 4. **Branen L, Hovgaard L, Nitulescu M, Bengtsson E, Nilsson J and Jovinge S**. Inhibition
355 of tumor necrosis factor-alpha reduces atherosclerosis in apolipoprotein E knockout mice.
356 *Arterioscler Thromb Vasc Biol* 24: 2137-2142, 2004.
357 5. **Buijs RM, van d, V, Garidou ML, Huitinga I and Escobar C**. Spleen vagal denervation
358 inhibits the production of antibodies to circulating antigens. *PLoS One* 3: e3152, 2008.
359 6. **Cailotto C, Costes LM, van d, V, van Bree SH, van Heerikhuizen JJ, Buijs RM and**
360 **Boeckstaens GE**. Neuroanatomical evidence demonstrating the existence of the vagal
361 anti-inflammatory reflex in the intestine. *Neurogastroenterol Motil* 24: 191-200, e93, 2012.
362 7. **Gallowitsch-Puerta M and Pavlov VA**. Neuro-immune interactions via the cholinergic
363 anti-inflammatory pathway. *Life Sci* 80: 2325-2329, 2007.
364 8. **Hansson GK and Libby P**. The immune response in atherosclerosis: a double-edged
365 sword. *Nat Rev Immunol* 6: 508-519, 2006.
366 9. **Hedblad B, Wikstrand J, Janzon L, Wedel H and Berglund G**. Low-dose metoprolol
367 CR/XL and fluvastatin slow progression of carotid intima-media thickness: Main results
368 from the Beta-Blocker Cholesterol-Lowering Asymptomatic Plaque Study (BCAPS).
369 *Circulation* 103: 1721-1726, 2001.
370 10. **Hu L, Boesten LS, May P, Herz J, Bovenschen N, Huisman MV, Berbee JF, Havekes**
371 **LM, van Vlijmen BJ and Tamsma JT**. Macrophage low-density lipoprotein receptor-
372 related protein deficiency enhances atherosclerosis in ApoE/LDLR double knockout mice.
373 *Arterioscler Thromb Vasc Biol* 26: 2710-2715, 2006.
374 11. **Huston JM, Ochani M, Rosas-Ballina M, Liao H, Ochani K, Pavlov VA, Gallowitsch-**
375 **Puerta M, Ashok M, Czura CJ, Foxwell B, Tracey KJ and Ulloa L**. Splenectomy
376 inactivates the cholinergic antiinflammatory pathway during lethal endotoxemia and
377 polymicrobial sepsis. *J Exp Med* 203: 1623-1628, 2006.
378 12. **Janig W**. Sympathetic nervous system and inflammation: a conceptual view. *Auton*
379 *Neurosci* 182: 4-14, 2014.
380 13. **Johansson ME, Ulleryd MA, Bernardi A, Lundberg AM, Andersson A, Folkersen L,**
381 **Fogelstrand L, Islander U, Yan ZQ and Hansson GK**. alpha7 Nicotinic acetylcholine
382 receptor is expressed in human atherosclerosis and inhibits disease in mice--brief report.
383 *Arterioscler Thromb Vasc Biol* 34: 2632-2636, 2014.
384 14. **Kleinbongard P, Heusch G and Schulz R**. TNFalpha in atherosclerosis, myocardial
385 ischemia/reperfusion and heart failure. *Pharmacol Ther* 127: 295-314, 2010.
386 15. **Kooijman S, Meurs I, van der Stoep M, Habets KL, Lammers B, Berbee JF, Havekes**
387 **LM, van EM, Romijn JA, Korpelaar SJ and Rensen PC**. Hematopoietic alpha7 nicotinic
388 acetylcholine receptor deficiency increases inflammation and platelet activation status, but
389 does not aggravate atherosclerosis. *J Thromb Haemost* 2014.
390 16. **Rezende AB, Neto NN, Fernandes LR, Ribeiro AC, Alvarez-Leite JI and Teixeira HC**.
391 Splenectomy increases atherosclerotic lesions in apolipoprotein E deficient mice. *J Surg*
392 *Res* 171: e231-e236, 2011.
393 17. **Robinette CD and Fraumeni JF, Jr**. Splenectomy and subsequent mortality in veterans of
394 the 1939-45 war. *Lancet* 2: 127-129, 1977.

- 395 18. **Rosas-Ballina M, Ochani M, Parrish WR, Ochani K, Harris YT, Huston JM, Chavan S**
396 **and Tracey KJ.** Splenic nerve is required for cholinergic antiinflammatory pathway control
397 of TNF in endotoxemia. *Proc Natl Acad Sci U S A* 105: 11008-11013, 2008.
- 398 19. **Rosas-Ballina M, Olofsson PS, Ochani M, Valdes-Ferrer SI, Levine YA, Reardon C,**
399 **Tusche MW, Pavlov VA, Andersson U, Chavan S, Mak TW and Tracey KJ.**
400 Acetylcholine-synthesizing T cells relay neural signals in a vagus nerve circuit. *Science*
401 334: 98-101, 2011.
- 402 20. **Shimada K, Hirano E, Kimura T, Fujita M and Kishimoto C.** Carvedilol reduces the
403 severity of atherosclerosis in apolipoprotein E-deficient mice via reducing superoxide
404 production. *Exp Biol Med (Maywood)* 237: 1039-1044, 2012.
- 405 21. **Ulleryd MA, Bernberg E, Yang LJ, Bergstrom GM and Johansson ME.** Metoprolol
406 reduces proinflammatory cytokines and atherosclerosis in ApoE-/- mice. *Biomed Res Int*
407 2014: 548783, 2014.
- 408 22. **van Diepen JA, Berbee JF, Havekes LM and Rensen PC.** Interactions between
409 inflammation and lipid metabolism: relevance for efficacy of anti-inflammatory drugs in the
410 treatment of atherosclerosis. *Atherosclerosis* 228: 306-315, 2013.
- 411 23. **Vida G, Pena G, Deitch EA and Ulloa L.** alpha7-cholinergic receptor mediates vagal
412 induction of splenic norepinephrine. *J Immunol* 186: 4340-4346, 2011.
- 413 24. **Wang H, Yu M, Ochani M, Amella CA, Tanovic M, Susarla S, Li JH, Wang H, Yang H,**
414 **Ulloa L, Al-Abed Y, Czura CJ and Tracey KJ.** Nicotinic acetylcholine receptor alpha7
415 subunit is an essential regulator of inflammation. *Nature* 421: 384-388, 2003.
- 416 25. **Westerterp M, van der Hoogt CC, de HW, Offerman EH, Dallinga-Thie GM, Jukema**
417 **JW, Havekes LM and Rensen PC.** Cholesteryl ester transfer protein decreases high-
418 density lipoprotein and severely aggravates atherosclerosis in APOE*3-Leiden mice.
419 *Arterioscler Thromb Vasc Biol* 26: 2552-2559, 2006.
- 420 26. **Wiklund O, Hulthe J, Wikstrand J, Schmidt C, Olofsson SO and Bondjers G.** Effect of
421 controlled release/extended release metoprolol on carotid intima-media thickness in
422 patients with hypercholesterolemia: a 3-year randomized study. *Stroke* 33: 572-577, 2002.
- 423 27. **Wong MC, van Diepen JA, Hu L, Guigas B, de Boer HC, van Puijvelde GH, Kuiper J,**
424 **van Zonneveld AJ, Shoelson SE, Voshol PJ, Romijn JA, Havekes LM, Tamsma JT,**
425 **Rensen PC, Hiemstra PS and Berbee JF.** Hepatocyte-specific IKKbeta expression
426 aggravates atherosclerosis development in APOE*3-Leiden mice. *Atherosclerosis* 220:
427 362-368, 2012.
- 428
429

430 **Figure legends**

431

432 **Figure 1. Confirmation of splenic denervations and gating strategy**

433 Schematic representation of the innervation of the spleen (**A**). The sympathetic input (pink)
434 reaches the spleen via the arteries, the parasympathetic input (green) reaches the spleen via
435 both tips of the spleen. The location at which denervations were performed are shown by the
436 dashed lines. Gating strategy for flow cytometry analysis (**B**). Confirmation of sympathetic
437 denervation (**C**) by measurement of tyrosine hydroxylase protein content of the spleen. As
438 controls, TH content for the brain and (denervated) brown fat are included.

439

440 **Figure 2. Effect of splenic denervation on immune cell composition of the spleen.**

441 APOE*3-Leiden.CETP mice were fed a WTD during 4 weeks, were randomized into three
442 groups receiving either splenic parasympathetic denervation (Px), sympathetic denervation (Sx),
443 or sham surgery (t=0). Mice were fed a WTD during 15 additional weeks before spleens were
444 isolated and cellular composition was analyzed by flow cytometry. Immune cells were counted
445 based on FSC (**A**) and further subdivided into B cells (CD19⁺) (**B**), T cells (CD3⁺) (**C**), dendritic
446 cells (CD11c⁺CD14⁻) (**D**), neutrophils (CD11b⁺Ly6G^{high}) (**E**) and monocytes/macrophages
447 (CD14⁺CD11b⁺) (**F**). Specific T cells subsets were identified as T_H (CD4⁺) (**G**), T_{Cyt} (CD8⁺) (**H**),
448 naïve T_H (CD4⁺CD62L⁺) (**I**), activated T_H (CD4⁺ CD25⁺) (**J**), naïve T_{Cyt} (CD8⁺CD62L⁺) (**K**) and
449 activated T_{Cyt} (CD8⁺ CD25⁺) (**L**). Values represent means ± SEM of 5 mice per group. *p<0.05,
450 **p<0.01 compared to sham surgery.

451

452 **Figure 3. Effect of splenic denervation on the gene expression of inflammatory genes.**

453 During the course of the experiment body weight was monitored (**A**). At 15 weeks after Px, Sx or
454 sham surgery, spleens were weighed (**B**) and splenic weight was expressed as percentage of
455 body weight (**C**), total RNA was extracted and expression levels of TNF α , IL-1 β and IL-6 were

456 determined by real-time PCR (D). Similarly, livers were weighed (E) and hepatic expression of
457 these genes was determined (F). Peritoneal leukocytes were isolated and gene expression was
458 quantified (G). Values represent means \pm SEM of 15 mice per group *p<0.05, **p<0.01,
459 ***p<0.01 compared to sham surgery.

460
461 **Figure 4. Effect of splenic denervation on white blood cell composition, serum cytokines**
462 **and plasma lipids.**

463 At 15 weeks after Px, Sx or sham surgery, blood was drawn and analyzed by flow cytometry.
464 Immune cells were counted (A) and further subdivided into B cells (CD19⁺) (B), T cells (CD3⁺)
465 (C), dendritic cells (CD11c⁺CD14⁻) (D), neutrophils (CD11b⁺Ly6G^{high}) (E) and monocytes
466 (CD14⁺CD11b⁺) (F). Serum cytokine levels of TNF α (G), IL-1 β (H) and IL-6 (I) were measured.
467 Plasma concentrations of total cholesterol (TC), phospholipids (PL) and triglycerides (TG) were
468 determined (J). The distribution of cholesterol over the different lipoproteins was determined by
469 fractionation of pooled plasma by FPLC (K). Serum E-selectin (L). Values represent means \pm
470 SEM of 5 (A-F) or 15 (G-L) mice per group.

471
472 **Figure 5. Effect of splenic denervation on atherosclerotic lesion size and composition.**

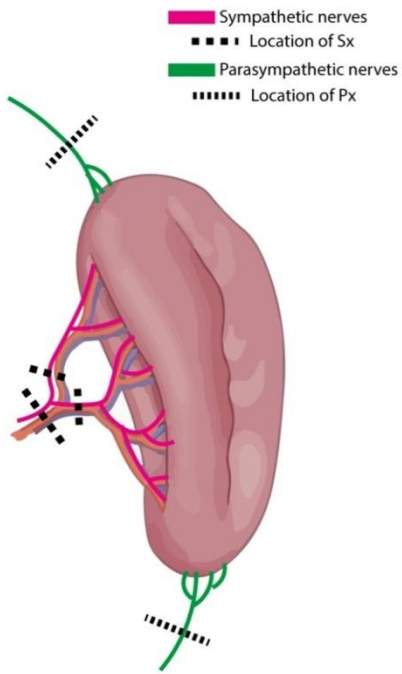
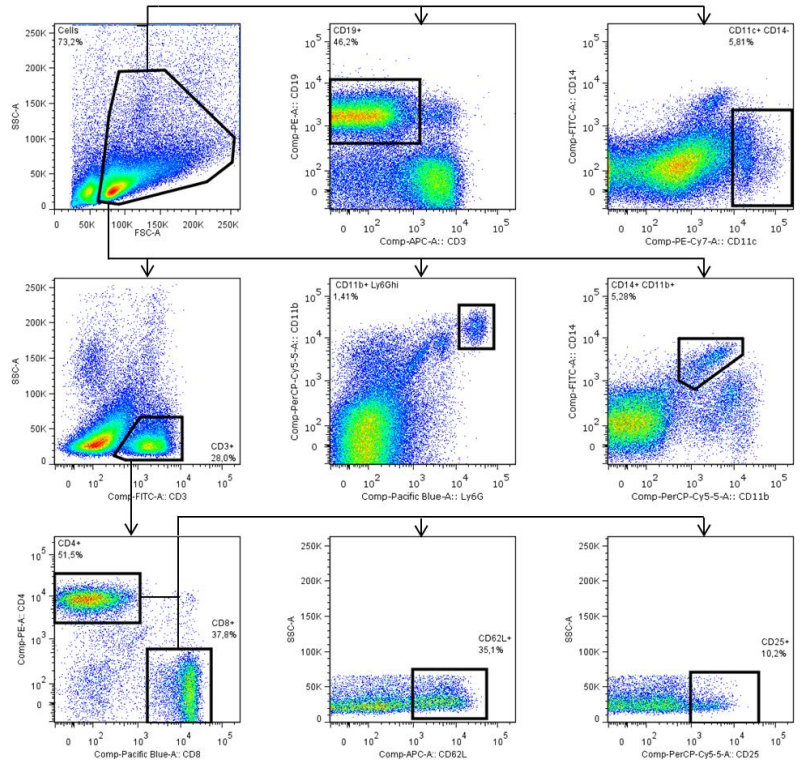
473 At 15 weeks after Px, Sx or sham surgery, hearts were isolated and cross-sections (5 μ m) with
474 50 μ m intervals throughout the aortic root area starting from the appearance of open aortic valve
475 leaflets were used for atherosclerosis measurements. Sections were stained with hematoxylin-
476 phloxine-saffron for histological analysis and representative images are shown (A).
477 Atherosclerotic mean lesion area (in μ m²) was quantified in four subsequent cross-sections (B).
478 The same four sections per mouse were categorized according to lesion severity (C). Lesion
479 composition was determined by immunohistochemistry in four subsequent cross-sections using
480 α -actin for smooth muscle cells (SMC) (D), Sirius Red staining for collagen content (E) and
481 MAC3 for macrophages (F). Values represent means \pm SEM of 15 mice per group.

482
483

Table 1: Detailed information of antibodies used for flow cytometry analysis.

Antibody	Conjugate	Clone	Source	Dilution
CD19	PE	ID3	BD	1,600
CD14	FITC	Sa14-2	eBioscience	500
CD11c	Biotin	HL3	BD	200
CD3	APC	145-2C11	BD	300
CD3	FITC	145-2C11	BD	400
CD11b	PerCP	M1/70	BD	800
Ly6G	Ef450	RB6-8C5	eBioscience	800
CD4	PE	L3T4 GK1.5	BD	1,000
CD8	biotin	53-6.7	BD	400
CD62L	APC	MEL-14	Biologend	1,600
CD25	PerCP	PC61	BD	500
Second step: Sav-PE-Cy7			BD	500

484
485
486
487

A**B****C****Figure 1**

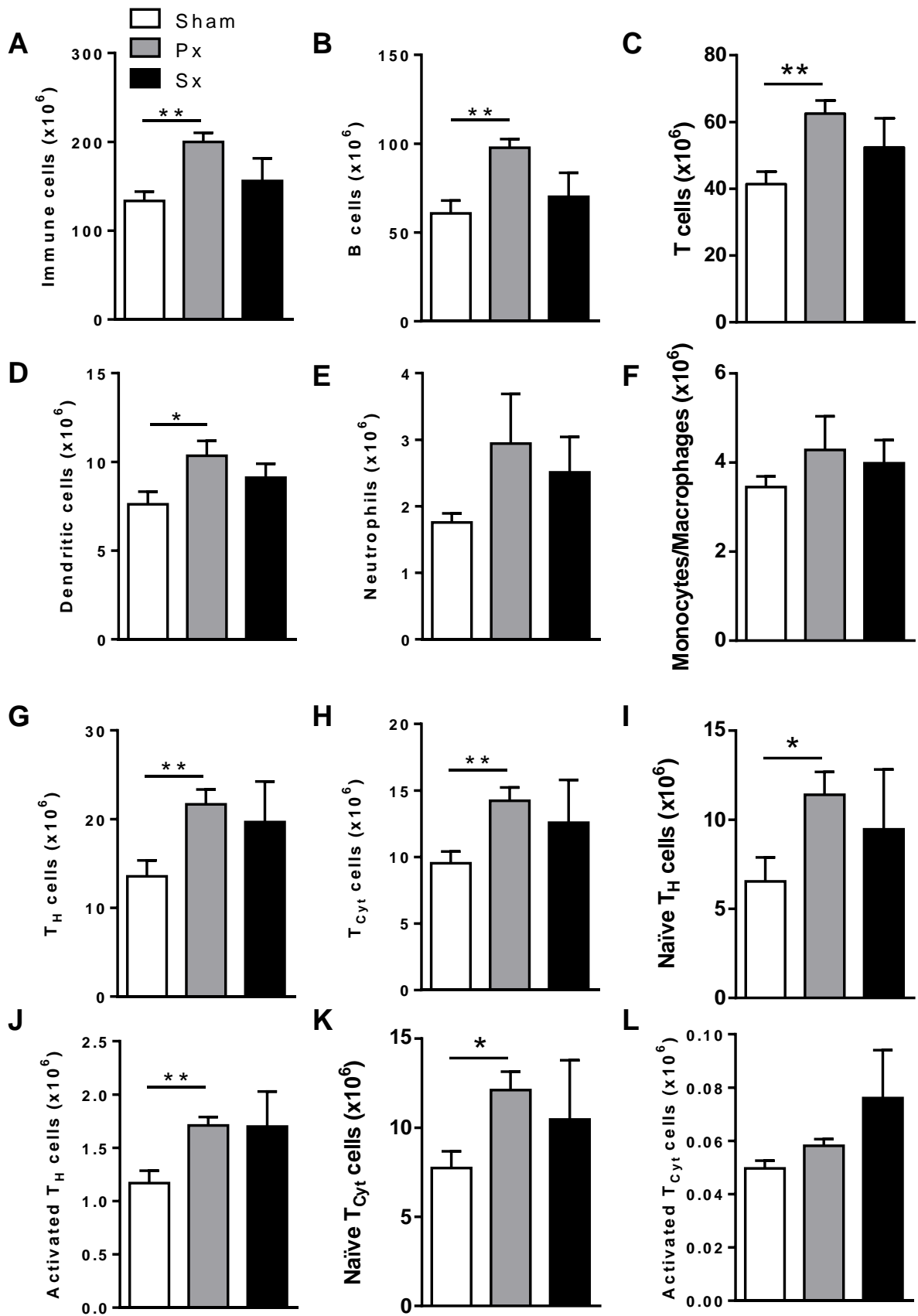


Figure 2

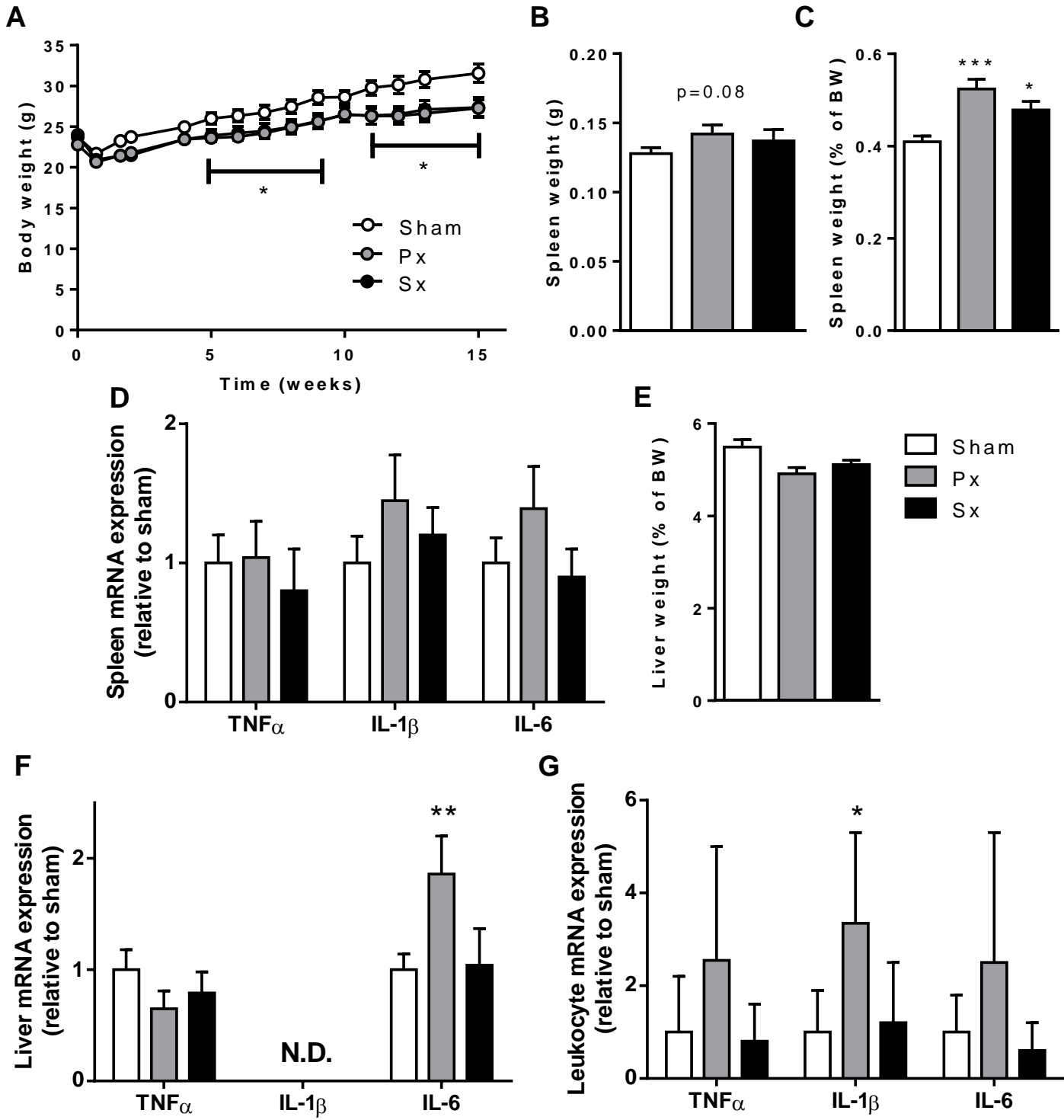


Figure 3

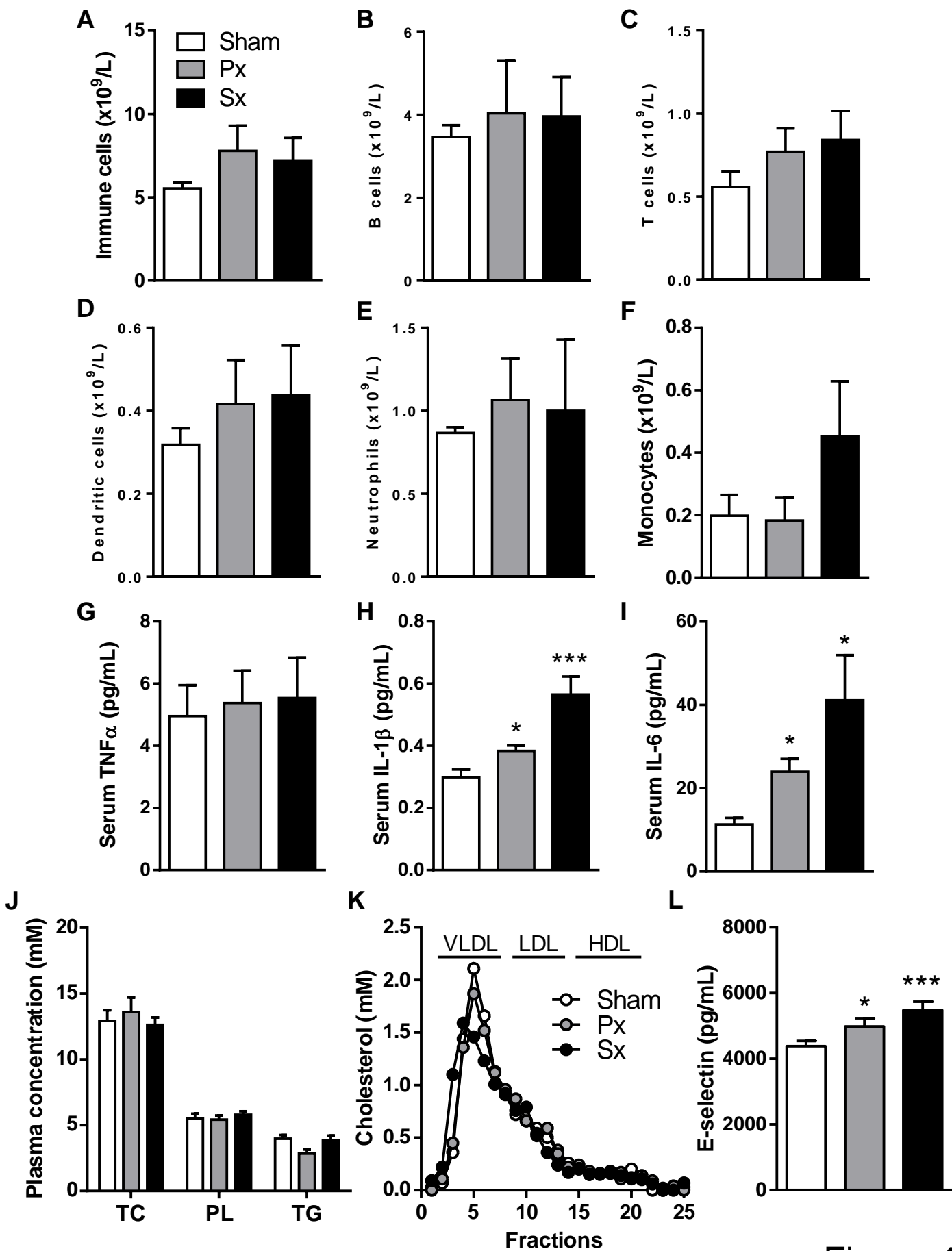


Figure 4

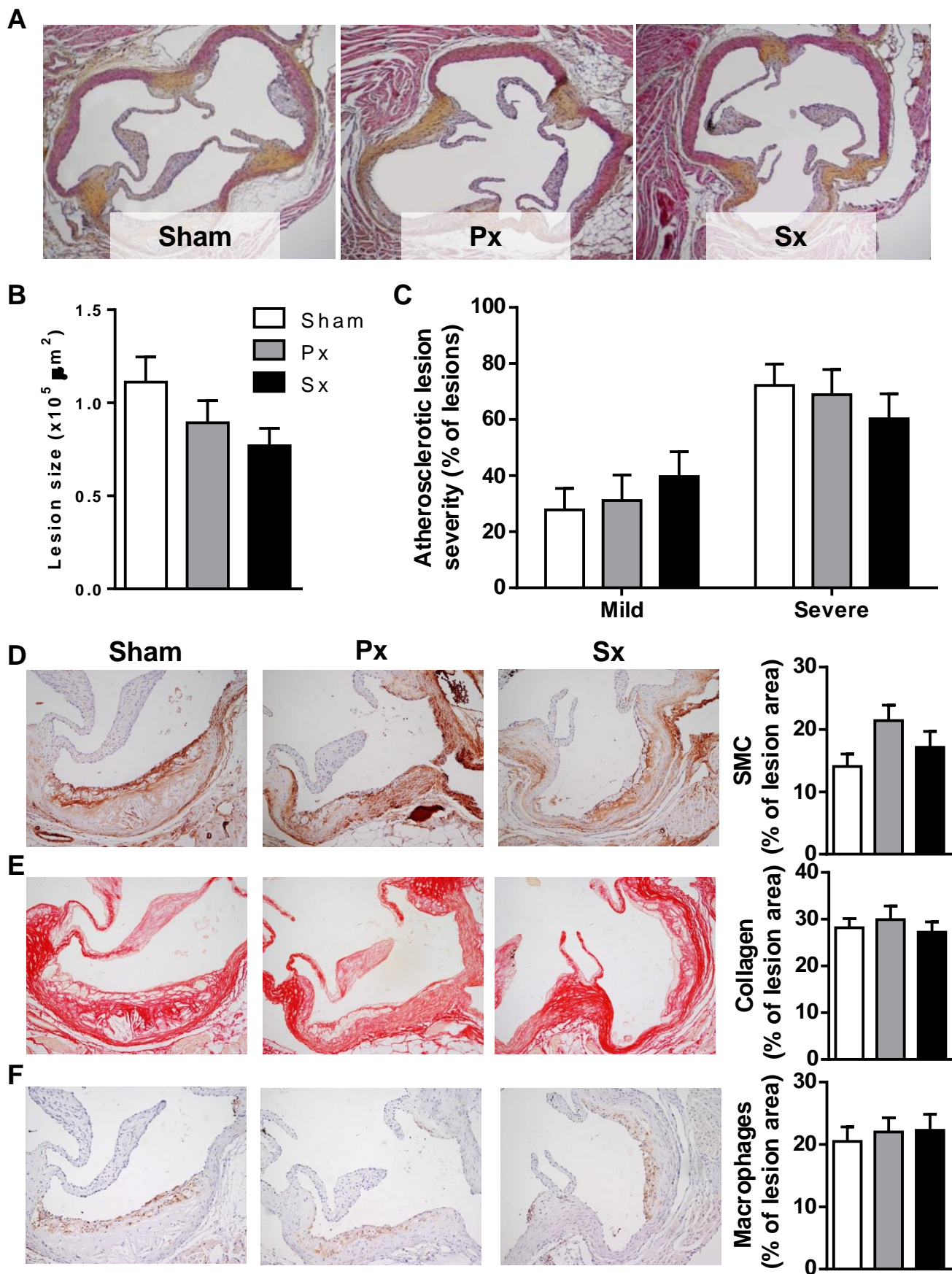


Figure 5